Single cell lineage tracing reveals a role for TgfβR2 in intestinal stem cell dynamics and differentiation

Jared M. Fischer[a,1], Peter P. Calabrese[b], Ashleigh J. Miller[a], Nina M. Muñoz[c], William M. Grady[d,e], Darryl Shibata[f], and R. Michael Liskay[a]

[a]Department of Molecular and Medical Genetics, Oregon Health and Science University, Portland, OR 97239; [b]Department of Molecular and Computational Biology, University of Southern California, Los Angeles, CA 90089; [c]Department of Interventional Radiology, University of Texas MD Anderson Cancer Center, Houston, TX 77030; [d]Clinical Research Division, Fred Hutchinson Cancer Research Center, Seattle, WA 98109; [e]Department of Medicine, University of Washington Medical School, Seattle, WA 98195; and [f]Department of Pathology, Norris Cancer Center, Keck School of Medicine, University of Southern California, Los Angeles, CA 90033

Edited by Elaine Fuchs, The Rockefeller University, New York, NY, and approved September 13, 2016 (received for review July 21, 2016)

Intestinal stem cells (ISCs) are maintained by a niche mechanism, in which multiple ISCs undergo differential fates where a single ISC clone ultimately occupies the niche. Importantly, mutations continually accumulate within ISCs creating a potential competitive niche environment. Here we use single cell lineage tracing following stochastic transforming growth factor β receptor 2 (*TgfβR2*) mutation to show cell autonomous effects of *TgfβR2* loss on ISC clonal dynamics and differentiation. Specifically, *TgfβR2* mutation in ISCs increased clone survival while lengthening times to monoclonality, suggesting that Tgfβ signaling controls both ISC clone extinction and expansion, independent of proliferation. In addition, *TgfβR2* loss in vivo reduced crypt fission, irradiation-induced crypt regeneration, and differentiation toward Paneth cells. Finally, altered Tgfβ signaling in cultured mouse and human enteroids supports further the in vivo data and reveals a critical role for Tgfβ signaling in generating precursor secretory cells. Overall, our data reveal a key role for Tgfβ signaling in regulating ISCs clonal dynamics and differentiation, with implications for cancer, tissue regeneration, and inflammation.

intestinal stem cell | Tgfβ | lgr5 | TgfβR2 | Paneth cell

The intestinal epithelium is constantly renewed by proliferating, multipotent, and self-renewing intestinal stem cells (ISCs) (1). There are two main populations of ISCs: (*i*) a proliferating ISC population that is important for homeostasis of the niche residing below the +4 position and expressing a set of markers [e.g., leucine-rich repeat-containing G-protein coupled receptor 5 (*Lgr5*) and *Olfm4*] and (*ii*) a quiescent ISC population residing near the +4 position and expressing a different set of markers (e.g., *Bmi1* and *Hopx*) (2). Proliferating ISCs are the workhorses during normal homeostasis and are maintained within the niche by a close relationship with Paneth cells (3) and the stroma (4). The proliferating ISC population can be further divided into a smaller number (4–8) of functional ISCs (5, 6), which are located at the bottom of the crypt and are biased toward survival within the niche (7). The proliferating ISCs use a population niche mechanism called neutral drift that combines differential ISC clone fates (8, 9). In neutral drift, a constant number of proliferative ISCs are maintained by a balance of ISC clone extinction with ISC clone expansion. Thus, the ISC niche must have signaling mechanisms that maintain and balance the different states of ISCs.

Much is known about the effects of WNT, BMP, and Notch signaling within the ISC niche (10), whereas little is known about the role that Tgfβ signaling through transforming growth factor β receptor 2 (*TgfβR2*) has on the ISC niche. Tgfβ signaling is known to play important roles in differentiation, cell motility, cell cycle, apoptosis, and inflammation (11), is critical during several phases of mammalian development (12–14), and is altered in cancer (15, 16). Tgfβ signaling involves Tgfβ ligands (Tgfβ1, 2, or 3) that bind to and activate Tgfβ receptors on the cell surface. The receptors, TgfβR1 and TgfβR2, form a heterodimer on ligand binding to create an active complex. The activated Tgfβ receptor complex phosphorylates and activates Smad2 and Smad3 (pSmad2/3), which in turn bind to Smad4, forming a transcriptional complex, which translocates to the nucleus and regulates target genes. Given the basic role of Tgfβ signaling within a cell, it seems likely that Tgfβ signaling will play a role within ISCs.

Previous investigations of *TgfβR2* mutation in the intestine using epithelium-wide deletion did not detect any obvious phenotypes (17–19). However, the design of these studies would not have detected phenotypes resulting from competition between Tgfβ-positive and -negative cells within the crypt. For example, there is evidence from the hematopoietic system that competition between cells with and without Tgfβ signaling resulted in a different phenotype compared with an environment with no competition (20). ISCs are constantly dividing and therefore continually accumulating diverse mutations, which can potentially result in competition-driven drift between ISCs. Recent studies have demonstrated that isolated single ISCs with mutations in *Kras* and *Apc* are more prone to clonal expansion relative to surrounding WT ISCs (21, 22). Here we examine the effects of stochastic loss of *TgfβR2* on competition between mutant and WT ISCs.

Results

Continuous and Pulse Labeling of ISCs Reveal Altered Clonal Dynamics Following *TgfβR2* Mutation. We used the stochastic $Pms2^{cre}$ system to determine the consequences of sporadic, low-frequency,

Significance

Although Tgfβ signaling is important in intestinal development and cancer, little is known about the consequences of sporadic transforming growth factor β receptor 2 (*TgfβR2*) mutation in intestinal stem cells (ISCs). By labeling single, *TgfβR2*-mutant ISCs, we measured the effects of *TgfβR2* loss on competition-driven clonal dynamics and differentiation. Specifically, we found that stochastic loss of *TgfβR2* increases clonal survival while paradoxically decreasing clonal expansion and crypt fission, further elucidating mechanisms responsible for the role of Tgfβ signaling in ISCs on tumor initiation and tissue regeneration. In addition, we found that Tgfβ signaling modulates the generation of secretory cell precursors, revealing a role for Tgfβ signaling in altering ISC differentiation with implications for cancer, tissue regeneration, and inflammation.

Author contributions: J.M.F., D.S., and R.M.L. designed research; J.M.F. and A.J.M. performed research; P.P.C., N.M.M., and W.M.G. contributed new reagents/analytic tools; J.M.F., P.P.C., A.J.M., D.S., and R.M.L. analyzed data; and J.M.F., D.S., and R.M.L. wrote the paper.

The authors declare no conflict of interest.

This article is a PNAS Direct Submission.

Data deposition: The sequences reported in this paper have been deposited in the Gene Expression Omnibus (GEO) database, www.ncbi.nlm.nih.gov/geo (accession nos. GSE58296 and GSE83423).

[1]To whom correspondence should be addressed. Email: fischerj@ohsu.edu.

This article contains supporting information online at www.pnas.org/lookup/suppl/doi:10.1073/pnas.1611980113/-/DCSupplemental.

single cell *TgfβR2* disruption in isolated crypts within the mouse small intestine (23–25). In our system, the $Pms2^{cre}$ allele is comprised of a revertible out-of-frame *cre* gene that is targeted to *Pms2*, a DNA mismatch repair gene expressed in multiple cell types, including ISCs. By using a stochastic process (spontaneous frame-shift mutation), activation of Cre recombinase occurs at a defined rate resulting in continuous labeling similar to another system (5) (Fig. S1*A*). Lineage labeling in the intestine will only be retained when *Cre* activation occurs in a long-lived progenitor cell (i.e., stem cell), thus making the $Pms2^{cre}$ mouse system ideal for continuous clonal labeling (Fig. 1*A*). When this system is combined with conditional *TgfβR2* alleles ($TgfβR2^{fx}$), we can monitor the fate of isolated ISCs in a niche with neutral drift (i.e., labeled WT ISC surrounded by unlabeled, WT ISCs) or in a niche with competition-driven drift (i.e., labeled TgfβR2-mutant ISC surrounded by unlabeled, WT ISCs).

Using the stochastic system described above, we compared proximal small intestines of $Pms2^{cre/cre}$; $TgfβR2^{+/+}$; *R26R* (WT) and $Pms2^{cre/cre}$; $TgfβR2^{fx/fx}$; *R26R* (TgfβR2 mutant) mice. First, we determined the number of partial and fully labeled β-gal$^+$ crypts at different ages. For simplicity, we divided the crypt into one-quarter fractions or clone sizes (Fig. 1*B*). For WT mice, we found a constant number of partially labeled crypts with age (average, 217 β-gal$^+$ foci) (Fig. 1*D*) and, as expected, an increasing number of fully labeled crypts with age (~4.1 β-gal$^+$ foci/d) (Fig. 1*C*). Interestingly, for TgfβR2-mutant mice, we found greater numbers of both partially labeled (average, 630 β-gal$^+$ foci; $P < 0.001$ for intercept) (Fig. 1*D*) and fully labeled crypts (~8.3 β-gal$^+$ foci/d; $P = 0.001$ for slope) compared with WT mice (Fig. 1*C*). The altered drift following *TgfβR2* loss in ISCs was independent of cell proliferation, apoptosis, or the total cell number within the crypt (Fig. S2 *A*–*C*). In addition, Tgfβ-responsive cells, as measured by pSmad2/3 staining, were evenly distributed throughout the crypt bottom (Fig. S2*D*). These results are consistent with TgfβR2-mutant ISCs having greater competition-driven clonal survival (more fully labeled crypts with age) while also having an elongated time to full crypt occupancy (more partially labeled crypts) compared with labeled, WT ISCs.

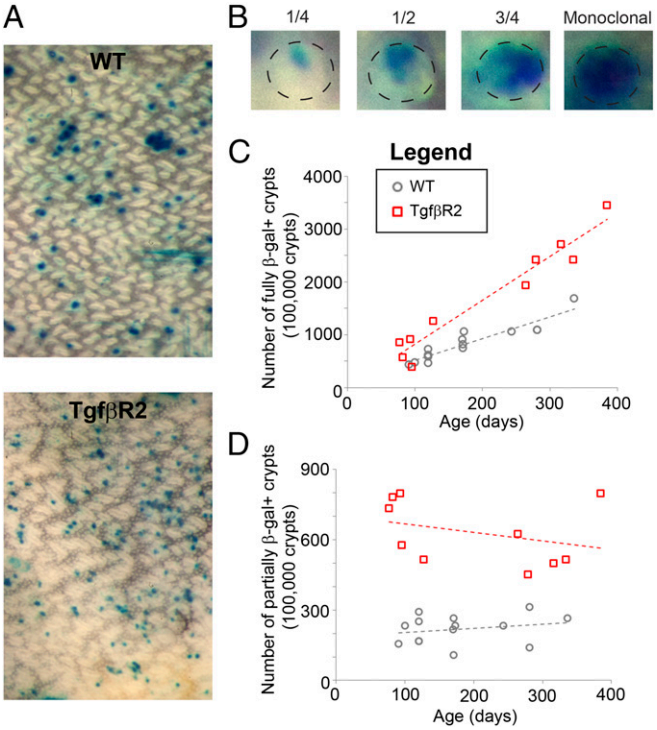

Fig. 1. Continuous clonal labeling ($Pms2^{cre}$) following stochastic loss of *TgfβR2*. (*A*) Images of the small intestine from WT (281 d old) and TgfβR2-mutant (279 d old) mice showing β-gal$^+$ crypts. (*B*) Images of partially (1/4, 1/2, 3/4) and fully (monoclonal) β-gal$^+$ crypts. (*C*) Fully labeled crypts plotted with age. TgfβR2-mutant intestine have increased accumulation of fully β-gal$^+$ crypts compared with WT. Dashed lines are linear regressions. (*D*) Partially labeled crypts plotted with age. TgfβR2-mutant intestine have more partially β-gal$^+$ crypts compared with WT. Dashed lines are linear regressions. Each spot is an independent mouse and at least 9,000 total crypts were analyzed per mouse. See also Figs. S1–S3.

We verified Cre-mediated recombination of the *TgfβR2* floxed allele by PCR assay on microdissected crypts and found that 92% (23/25) of β-gal$^+$ foci were positive for *TgfβR2* recombination, whereas only 10% (1/10) of β-gal^{neg} foci were positive for *TgfβR2* recombination ($P < 0.001$; Fig. S3*A*). The PCR data strongly support efficient recombination of *TgfβR2* in β-gal$^+$ cells and the stochastic nature of the $Pms2^{cre}$ system with a calculated β-gal$^+$ activation rate of 0.0003 β-gal$^+$ events per cell (Fig. S3*C*), making multiple, independent *TgfβR2* mutations in a single crypt highly unlikely. In addition, we found pSmad2/3$^+$ cells in 15% (151/1,028) of β-gal^{neg} crypts, but only in 4% (15/404) of β-gal$^+$ crypts from $TgfβR2^{fx/fx}$ mice, supporting loss of Tgfβ signaling in 75% [1 − (observed/expected)] of β-gal$^+$ crypts. Therefore, the data for β-gal$^+$ cells in the TgfβR2-mutant mice are representative of a single *TgfβR2* mutant ISC arising within a crypt of WT ISCs.

To determine independently the consequences of eliminating Tgfβ signaling in proliferating ISCs, we used *Lgr5-CreER* mice with, or without, conditional *TgfβR2* alleles. The *Lgr5-CreER* mouse contains Cre fused to the estrogen receptor and is expressed from the ISC-specific promoter, *Lgr5* (26). Thus, after injection of tamoxifen (pulse labeling), Cre becomes active in ISCs and, when combined with a *LacZ* reporter allele (*R26R*), can label the ISC for lineage tracing (Fig. 2*A*). By labeling a small number of ISCs in any given crypt, we can follow the progression of a crypt from partially labeled to fully labeled (time to monoclonality) and the fraction of surviving β-gal$^+$ crypts (crypt succession) (Fig. S1*B*). To study drift, we compared the clone size distribution or crypt succession with time in *Lgr5-CreER*; $TgfβR2^{+/+}$; *R26R* (WT) and *Lgr5-CreER;* $TgfβR2^{fx/fx}$; *R26R* (TgfβR2-mutant) mice, injected with tamoxifen at 2 mo of age. By using a single dose of tamoxifen (2 mg/mouse), we were able to induce mosaic recombination in a fraction of crypts (~20%) while still obtaining recombination of the $TgfβR2^{fx}$ alleles (Fig. S3*A*). The dose of tamoxifen used can result in multiple, recombination events per crypt (Fig. S3*B*); therefore, it is possible to have β-gal^{neg} and β-gal$^+$; TgfβR2-mutant ISCs within a single crypt. For pulse labeling, clonal survival was increased in TgfβR2-mutant crypts compared with WT crypts (Fig. 2*B*) ($P = 0.02$ for log-transformed slope). In addition, the time to monoclonality was elongated in TgfβR2-mutant crypts compared with WT crypts (Fig. 2*C*) ($P < 0.001$ for logit-transformed slope). These results are again consistent with TgfβR2-mutant ISCs having greater competition-driven clonal survival (more labeled crypts) while also having an elongated time to full crypt occupancy (longer time to monoclonality) compared with β-gal$^+$, WT ISCs.

Computational Simulations Reveal Both Decreased ISC Clone Expansion and Clone Extinction Following Stochastic Loss of *TgfβR2*. To interpret how the changes in ISC clone survival and times to monoclonality affect ISC clonal dynamics, we simulated competition between WT and mutant ($TgfβR2^{-/-}$) ISCs. Our model has the following parameters: N (number of stem cells), m (mutation rate), time, λ (WT replacement rate), TgfβR2-λ ($TgfβR2^{-/-}$ replacement rate), and F_R ($TgfβR2^{-/-}$ replacement factor) (Fig. S4*A*). Our model is independent of cell proliferation; however, *TgfβR2* loss did not have any appreciable effect on proliferation in cells located at the crypt base (Fig. S2*A*). Simplistically, the fate of an isolated single ISC depends on the relative balance between clone extinction vs.

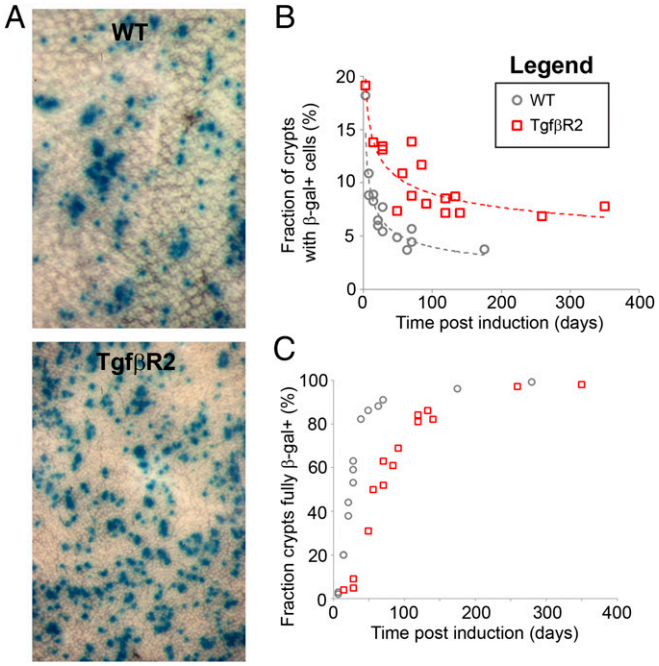

Fig. 2. Pulse labeling (*Lgr5-CreER*) following stochastic loss of *TgfβR2*. (*A*) Images of the small intestine from WT (49 d after induction) and TgfβR2-mutant (56 d after induction) mice showing β-gal$^+$ crypts. (*B*) The number of remaining β-gal$^+$ crypts was increased in TgfβR2-mutant intestine compared with WT. Dashed lines are exponential trend lines. (*C*) Time to monoclonality was elongated in TgfβR2-mutant crypts compared with WT. Each spot is an independent mouse and at least 9,000 total crypts were analyzed per mouse. See also Figs. S1 and S3.

clone expansion, where λ reflects the rate of ISC clone extinction, whereas F_R reflects the rate of competitive ISC clone expansion.

First, we calculated N and λ for WT crypts using our computational model with both the continuous and pulse labeling, which revealed that the best fit for WT crypts was $N = 4$ and λ = 0.14–0.15 (Table S1 and Fig. S5 *A* and *C*), similar to a previous estimate (5). Next, we calculated the effects of *TgfβR2* mutation on ISC competition-driven drift. These simulations revealed an approximately sevenfold decreased clone extinction (TgfβR2-λ) and an approximately threefold decreased competitive clone expansion (F_R) (Fig. S4 *B* and *C* and Table S1). These simulations indicate an approximately twofold greater reduction in ISC clone extinction compared with clone expansion following loss of *TgfβR2* when in competition with WT ISCs, leading to the slower but overall increased niche occupancy. The net result is that *TgfβR2*-mutant ISCs have increased clone survival compared with WT ISCs. Because ISC proliferation is not altered with *TgfβR2* mutation, these results suggest that the increased clone survival of *TgfβR2*-mutant ISCs is through altered differentiation.

Loss of *TgfβR2* in ISCs in Vivo Reduces the Chance of Crypt Fission. Our data revealed that loss of *TgfβR2* could lengthen times to monoclonality, supporting reduced ISC clone expansion. Next, we examined the effects of stochastic mutation on crypt fission, the process by which a single crypt splits into two crypts presumably caused by an increased number of ISCs (i.e., ISC clone expansion). The stochastic nature of the *Pms2^{cre}* system make multiple, independent *TgfβR2* mutations in neighboring crypts highly unlikely; thus, the distribution of crypt patch sizes reflects crypt fission events over time. Therefore, we determined the numbers of β-gal$^+$ foci that contain multiple, neighboring β-gal$^+$ crypts in similarly aged WT (mean, 192 d) or TgfβR2-mutant (mean, 192 d) mice (P = 0.99). Interestingly, there was an overall reduced size of β-gal$^+$ foci in TgfβR2-mutant intestines (mean β-gal$^+$ focus size = 1.5 crypts) compared with WT intestines (mean β-gal$^+$ focus size = 1.9 crypts), suggesting reduced crypt fission in TgfβR2-mutant crypts (P = 0.003; Fig. 3*A*). These results are consistent with decreased crypt fission following stochastic *TgfβR2* mutation.

Next, we combined the *Villin-Cre* allele with conditional *TgfβR2^{fx}* alleles (*TgfβR2^{IEKO}*) (17, 19, 27) to determine whether the effects of *TgfβR2* loss on crypt fission were caused by competition with WT cells or by TgfβR2-mutant crypts inherently having a reduced level of crypt fission. The *TgfβR2^{IEKO}* mice exhibit loss of *TgfβR2* throughout the intestinal epithelium; thus, almost all epithelial cells (and crypts) become *TgfβR2$^{-/-}$* without intra- or inter-crypt competition. Previous reports on these mice did not report any obvious differences from the intestines of WT mice; however, there was not a close examination of crypt fission rates (17, 19, 27). Therefore, we examined the number of crypts undergoing fission (crypts in the process of budding) in adult *TgfβR2^{IEKO}* (mean, 16 mo) or WT (mean, 15.4 mo) mice (P = 0.76). Interestingly, we found a reduced percentage of crypts undergoing fission in *TgfβR2^{IEKO}* intestine compared with WT intestine (Fig. 3*B*). These results revealed that TgfβR2-mutant crypts inherently have reduced crypt fission whether in competition with neighboring crypts or not.

Loss of *TgfβR2* in ISCs in Vivo Reduces the Chance of Regeneration Following Irradiation. Next, we studied the effects of irradiation following sporadic loss of *TgfβR2* in ISCs because ISC clonal expansion is necessary following crypt damage, and our data suggest that *TgfβR2* loss retards ISC clonal expansion. A subset of Lgr5$^+$ ISCs is necessary for crypt regeneration following irradiation (28), and intestine-wide loss of *TgfβR2* resulted in a slower rate of crypt regeneration following irradiation (27). Therefore, we studied the effects of irradiation (12 Gy) on TgfβR2-mutant ISCs when competing with WT ISCs using the pulse labeling model (*Lgr5-CreER* mice). We define β-gal$^+$ foci that extend from the crypt onto the body of the villus as a "repopulated clone" and β-gal$^+$ foci that were only present on the body of the villus (not extending into the crypt) as an "extinguished clone." Mice were given a single pulse of tamoxifen and then 3 wk later were exposed to 12 Gy of irradiation. Five to 7 d after irradiation, TgfβR2-mutant cell lineages in the proximal small intestine were scored as repopulated clones in only 35% of crypts compared with 66% in WT cell lineages (Fig. 3*C*). Finally, we found that irradiation altered the distribution of pSmad2/3$^+$ cells toward the crypt base (Fig. S2*D*) and dramatically increased the pSmad2/3 staining intensity and number (~20-fold) of pSmad2/3$^+$ cells within the crypt, specifically in the Paneth cell lineage (Fig. 3*D*). However, there was minimal change in the number of pSmad2/3$^+$ cells in the stroma after irradiation (Fig. 3*D*). These data support a key role for Tgfβ signaling through *TgfβR2* within the ISC population in crypt regeneration after damage and a role for Tgfβ signaling in the Paneth cell lineage.

Cell Type Analysis in Vivo Reveals a Role for TgfβR2 in the Generation of Paneth Cells. Because our data suggested a role for Tgfβ signaling in differentiation, we examined *Pms2^{cre}* mice for altered cell labeling after *TgfβR2* deletion. We found that 21% of β-gal$^+$ crypts from TgfβR2-mutant mice showed an absence of β-gal$^+$ cells characteristic of Paneth cells compared with only 1% of β-gal$^+$ crypts in WT mice (P = 0.03; Fig. 4*A*). We also analyzed *Lgr5-CreER* mice and noted that, at 4 wk following *TgfβR2* loss, there was an average of 5.9 ± 0.4 β-gal$^+$ Paneth cells in WT crypts, but only an average of 3.5 ± 0.4 β-gal$^+$ Paneth cells in TgfβR2-mutant crypts (P = 0.002). These results suggest that TgfβR2-mutant ISCs are less likely to generate Paneth cells than WT ISCs.

To study further the effects of *TgfβR2* loss on differentiation, we used the *TgfβR2^{IEKO}* mice (17, 19) to determine whether the effect of *TgfβR2* loss on the formation of Paneth cells was caused by competition with WT cells or by an inherent defect of TgfβR2-mutant crypts. Interestingly, we observed 18% fewer Paneth cells per crypt section in *TgfβR2^{IEKO}* mice compared with *TgfβR2^{fx}* mice

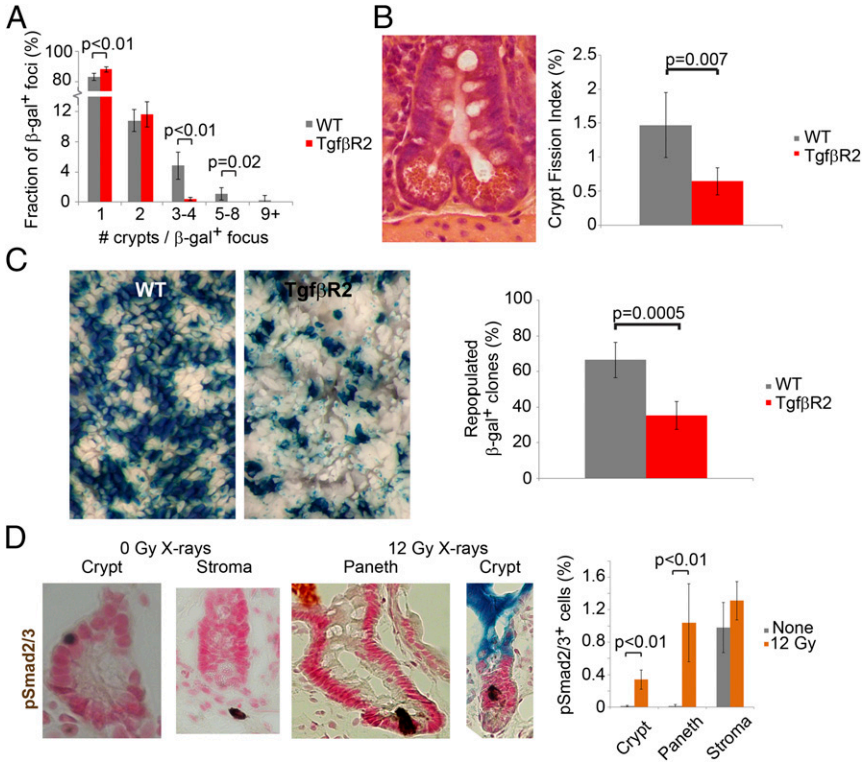

Fig. 3. Crypt fission and regeneration are reduced following loss of *TgfβR2* in ISCs. (*A*) Using continuous clonal labeling, we observed a reduced fraction of larger β-gal$^+$ foci (3+ neighboring β-gal$^+$ crypts) in TgfβR2-mutant intestine (n = 5 mice) compared with WT intestine (n = 6 mice). (*B*) Image of a crypt undergoing fission. Graph showing reduced crypt fission index in intestines with intestine-wide deletion of *TgfβR2* (n = 5 mice) compared with WT crypt fission index (n = 9 mice). (*C*) Images of stained intestine from WT or TgfβR2-mutant mice with pulse labeling and irradiation (12 Gy). Decreased number of repopulated β-gal$^+$ clones following irradiation in TgfβR2-mutant intestine (n = 6 mice) compared with WT intestine (n = 4 mice). (*D*) Immunohistochemistry for pSmad2/3 in unirradiated and irradiated intestine. Irradiation (12 Gy of X-rays) (n = 4 mice) increased the fraction of pSmad2/3$^+$ cells within the crypt, and specifically within Paneth cells, compared with unirradiated control intestine (n = 8 mice). No significant change in the number pSmad2/3$^+$ stromal cells. Error bars are 1 SD.

($P < 0.001$; Fig. 4*B*). Overall, our results are consistent with *TgfβR2*-mutant ISCs possessing a reduced capacity to produce Paneth cells and thus a role for Tgfβ signaling in differentiation toward the secretory lineage.

Cultured Intestinal Enteroids Reveal a Role for Tgfβ Signaling in ISC Clonal Expansion. To study further the effects of Tgfβ signaling modifications on the intestinal epithelium, we used cultured mouse proximal small intestinal enteroids, which are self-perpetuating and capable of producing each of the cell types characteristic of the intestinal epithelium (29). The enteroids allow us to study the early and rapid effects of both up- and down-regulating Tgfβ signaling by treating with either an inhibitor of TgfβR1/2 (30) or Tgfβ1 ligand. Intestinal enteroids treated with high levels of Tgfβ1 ligand (4 ng/mL) results in cell death as seen previously (31) and could be rescued by cotreatment with the inhibitor of TgfβR1/2 (Fig. S6*A*). Because initial treatment with 4 ng/mL of Tgfβ1 ligand resulted in rapid enteroid death, we treated enteroids with the highest dose that did not induce enteroid death (0.04 ng/mL Tgfβ1 ligand; Fig. S6*A*). Although Tgfβ responsive cells (pSmad2/3$^+$) were rare (<3% of all cells) in both untreated and 0.04 ng/mL Tgfβ1-treated enteroids, Tgfβ1 treatment resulted in an approximately ninefold increased fraction of pSmad2/3$^+$ cells compared with untreated (P = 0.003; Fig. S7*A*), suggesting this level of Tgfβ1 ligand increases Tgfβ signaling but only in a limited number of cells.

To identify global changes in enteroids after altering Tgfβ signaling, we used Gene Set Enrichment Analysis (GSEA) (32) to determine if our treatment groups had similar gene expression enrichment for stem cell genes by comparing Lgr5-GFP^{high} cells with Lgr5-GFP^{low} cells (33). GSEA on the microarray data showed that the Tgfβ inhibitor resulted in decreased expression of genes characteristic of stem cells, whereas Tgfβ ligand treatment showed increased expression of the same genes from stem cells (Fig. 5*A*). In support of a reduced stem cell signature with Tgfβ inhibition, we observed a reduced rate of crypt bud formation following treatment of enteroids with the TgfβR1/2 inhibitor (Fig. 5*B*). Treatment with either the TgfβR1/2 inhibitor or 0.04 ng/mL Tgfβ1 ligand had no detectable effect of proliferation within the crypt bud (where the ISCs are located), but dramatically decreased proliferation outside of the crypt bud (Fig. S6*B*). These results further support the in vivo data that Tgfβ signaling does not affect ISC division rates, but instead support that the effects Tgfβ signaling are on ISC dynamics and clonal expansion.

Cultured Intestinal Enteroids Reveal a Role for Tgfβ Signaling in Differentiation Toward Secretory Cell Lineage Precursors. To determine whether altered Tgfβ signaling had gene expression enrichment for secretory precursor cell genes, we again started by using GSEA (32) and comparing secretory progenitors with enterocytes (34). GSEA on the microarray data showed that the Tgfβ inhibitor resulted in decreased expression of genes characteristic of secretory precursor cells, whereas Tgfβ ligand treatment showed increased expression of the same genes (Fig. 5*C*). To confirm the expression array data, we stained for the lectin from *Ulex europaeus* (UEA), which is a marker for the secretory cell lineage: Paneth, enteroendocrine, and Goblet cells (35). We found that the low dose of Tgfβ1 ligand resulted in an increased number of UEA$^+$ cells per bud (equivalent to the crypt), whereas treatment of the enteroids with the TgfβR1/2 inhibitor resulted in a decreased number of UEA$^+$ cells per bud (Fig. S7*B*). These data in intestinal enteroids support the in vivo data that Tgfβ signaling is key for differentiation toward the secretory cell lineage.

To study further the role of Tgfβ signaling in differentiation toward the secretory lineage, we altered Tgfβ signaling in combination with inhibiting Notch signaling, which is known to be critical for formation of the secretory cell lineage (36). We pretreated enteroids with either the Tgfβ1 ligand or TgfβR1/2 inhibitor for 2 d and then cotreated with the γ-secretase inhibitor DAPT for 4 d. Enteroids were examined for expression of the secretory cell marker gene, lysozyme, and a control gene, GAPDH, via qRT-PCR. In agreement with the microarray data, lysozyme expression was increased in enteroids treated with Tgfβ1 ligand (1.7-fold) and decreased with Tgfβ inhibition (0.2-fold). As expected, we found

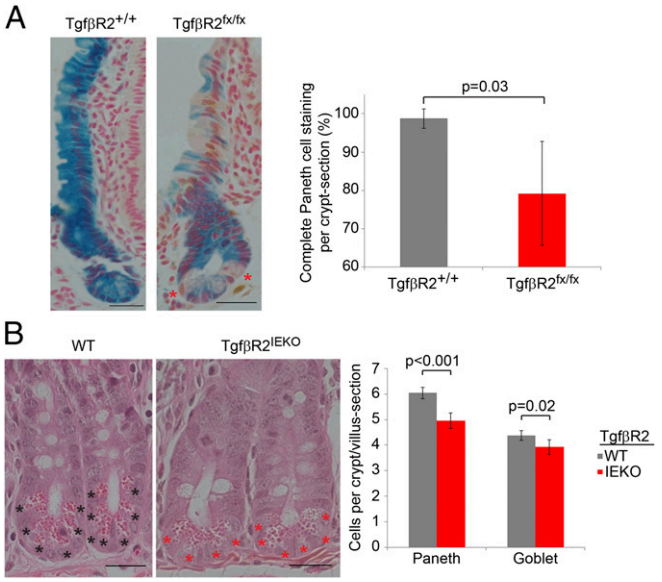

Fig. 4. Change in the formation of Paneth cells following deletion of *TgβR2* in vivo. (*A*) *Pms2*^{cre} mice revealed a reduced rate of Paneth cell generation following *TgfβR2* deletion in ISCs ($n = 4$ mice) compared with control, WT ISCs ($n = 4$ mice). Red asterisks mark unlabeled Paneth cells. (*B*) Intestinal epithelium wide deletion of *TgfβR2* (IEKO) resulted in significantly fewer cells of the secretory lineage (Paneth and Goblet) in crypts ($n = 5$ mice) compared with control, WT crypts ($n = 5$ mice). (Scale bar, 25 μm.) Error bars are 1 SD.

that DAPT treatment had a dramatic increase (sevenfold) on lysozyme expression in control enteroids (Fig. 5*D*). Interestingly, the combination of Tgfβ1 and DAPT treatment exponentially increased the expression of lysozyme (40-fold) in enteroids compared with control enteroids (Fig. 5*D*). These data suggest that Tgfβ signaling is acting on a precursor secretory cell lineage or ISC, which facilitates rapid formation of secretory cells when Notch signaling is inhibited.

Cultured Human Intestinal Enteroids Reveal a Role for Tgfβ Signaling in ISC Dynamics and Differentiation Toward Secretory Cell Lineage. To determine the relevance of these findings to human intestine, we cultured enteroids from a normal human duodenum. We found that increasing Tgfβ signaling increased GSEA for stem cell genes and secretory precursor cell genes (Fig. S8*A*) and increased the rate of new crypt bud formation (Fig. S8*B*). With time in culture, human enteroids progress from the budding phenotype to a more cyst-like phenotype. Notch inhibition (DAPT) alone dramatically increased the rate of invagination, which is an initial step in creating buds (Fig. S8*C*). Interestingly, the combination of DAPT and Tgfβ1 ligand treatment increased the number of invaginated enteroids compared with the DAPT-treated enteroids (Fig. S8*C*), supporting a role for Tgfβ signaling in conjunction with Notch inhibition in differentiation. These data are in agreement with our findings in mice and suggest that Tgfβ signaling is important in regulating stem cell dynamics and differentiation toward a precursor secretory cell lineage in human small intestinal epithelium.

Cultured Intestinal Enteroids Reveal a Role for Tgfβ Signaling in Regeneration After Damage. To study further the effects of altering Tgfβ signaling on crypt regeneration, we treated enteroids with either the Tgfβ inhibitor or ligand and the cytotoxic agent, FUDR (5-fluoro-2′-deoxyuridine), which kills proliferating cells (37). We pretreated enteroids for 3 d with the TgfβR1/2 inhibitor or Tgfβ1 ligand and then added FUDR for 1 d and allowed the enteroids to recover for 2 d. We found that altering the Tgfβ pathway alone had minimal impact on enteroid survival. However, when treated with FUDR, the TgfβR1/2 inhibitor pretreated enteroids showed decreased survival, whereas survival was increased in the enteroids pretreated with Tgfβ1 ligand (Fig. S9). These results again support the in vivo data that Tgfβ signaling has a role in crypt regeneration.

Discussion

Multiple mammalian ISCs within each crypt are maintained by a population niche mechanism of ISC clone expansion and extinction, ultimately resulting in neutral drift (8, 9). These differentially fated ISCs provide flexibility because any ISC clone extinction is readily compensated by neighboring ISC clone expansion. Although neutral drift is normally random, mutations within ISCs can alter clonal dynamics and induce selection as shown previously in ISCs with sporadic *Apc* or *Kras* mutations (21, 22). Here, we demonstrate that ISC clonal dynamics can be modulated genetically by mutations in *TgfβR2*. Specifically, stochastic loss of *TgfβR2* resulted in increased ISC clone survival compared with WT ISCs, but at the cost of clone expansion. In combination with the effects on ISC clonal dynamics, our data in vivo and in cultured enteroids strongly implicate Tgfβ signaling in the transition from ISC to a precursor secretory cell lineage. Thus, when an ISC receives Tgfβ signaling and transitions toward the secretory lineage, the end result for that ISC clone is extinction. Importantly, our data also suggest that Tgfβ signaling and thus precursor secretory cells are important in clone expansion, crypt fission, and ISC regeneration.

Here, we show that *TgfβR2* plays an important role in maintenance of the ISC clonal dynamics, which has important implications for cancer, tissue regeneration, and inflammation. First, the

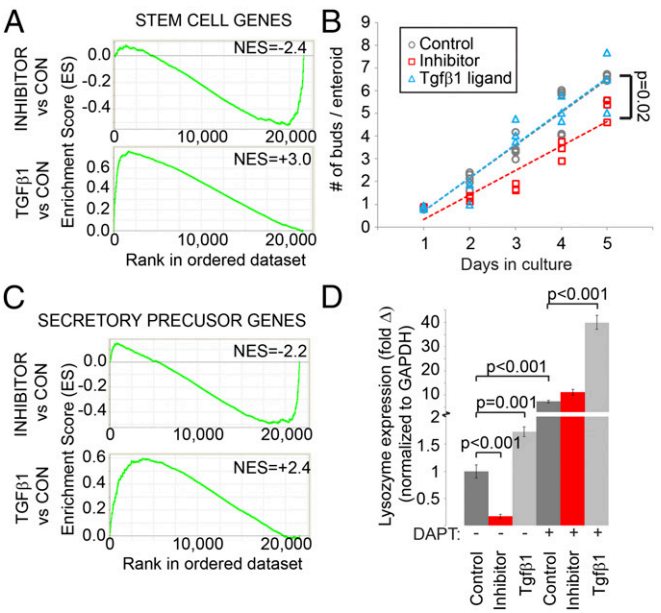

Fig. 5. Tgfβ signaling is important for the generation of stem and secretory cell lineage in cultured enteroids. (*A* and *C*) GSEA for Tgfβ inhibitor or Tgfβ1 ligand vs. control treatment. Tgfβ inhibitor treatment decreases the enrichment score (ES) for (*A*) stem cell and (*C*) secretory precursor genes ($P < 0.001$ for each). Tgfβ1 treatment increases the ES for (*A*) stem cell and (*C*) secretory precursor genes ($P < 0.001$ for each). NES, normalized enrichment score. (*B*) Enteroids treated with the TgfβR1/2 inhibitor show a slower accumulation of new crypt-bud formation compared with control or Tgfβ1 ligand treatment ($P = 0.02$ for slope). (*D*) Lysozyme expression measured by qRT-PCR is reduced with Tgfβ inhibition and increased with Tgfβ1 ligand compared with control treatment. In addition, Notch inhibition (DAPT treatment) greatly increases lysozyme expression, but the addition of Tgfβ1 ligand exponentially increases lysozyme expression compared with the control and Tgfβ inhibitor. ($n = 3$ for all treatment groups). Error bars are 1 SD. See also Figs. S6–S9.

increased ISC clone survival comes at the cost of reduced ISC clone expansion and crypt fission, which will hinder tumor initiation and progression. In contrast, stochastic mutations in *Apc* or *Kras* increase crypt fission and clonal expansion (21, 23–25). Thus, it is likely that the reduced ISC clonal expansion and crypt fission following *TgfβR2* mutation represents a key reason why *TgfβR2* mutations are rare early mutational events in sporadic CRC (38). Second, the decreased ISC clone expansion and crypt fission following sporadic *TgfβR2* mutations is detrimental to ISC and tissue regeneration following damage lending credence for why Tgfβ signaling is important for recovery after tissue damage (39, 40). Third, the correlation between Tgfβ signaling and formation of the secretory cell lineage has important implications in intestinal infection and inflammatory diseases. Specifically, Paneth cells maintain the homeostatic balance between the epithelium and the microbiota and are at the site of inflammation (41, 42). In conclusion, our data reveal the consequences of *TgfβR2* loss on ISC clonal dynamics and differentiation with implications for how mutation of *TgfβR2* can impact tissue homeostasis and alter tumorigenesis.

Methods

Complete materials and methods are reported in *SI Methods* and Table S2. All mouse experiments were approved by the Institutional Animal Care and Use Committee at Oregon Health and Science University. Intestines were stained for β-gal activity as previously described (25). Human duodenum was obtained with institutional review board approval at OHSU. Enteroids were treated with 20 μM LY2109761 (TgfβR1/2 inhibitor) (Adooq) (30) or 0.04 ng/mL (unless specified differently) Tgfβ1 ligand (R&D Biosystems). The computational model is a continuous-time, asynchronous model with a constant number of stem cells (*N*), modified from a previous model (22). To calculate statistical significance, we used univariate linear regressions in StatistiXL on both datasets (WT and mutant) and compared the slopes of each regression with ANOVA.

ACKNOWLEDGMENTS. We thank Dr. Jessica Minnier for help with statistical analyses; Dr. Jason Link for human duodenal samples; and Drs. Doug Winton, Melissa Wong, Nick Smith, Thomas Doetschman, and James Stringer for critical comments on the manuscript. Microarray assays were performed in the OHSU Gene Profiling Shared Resource. J.M.F. was funded by NIH Grant 1K99CA181679, Clinical and Translational Science Awards Grant UL1TR000128, and the Medical Research Foundation of Oregon. R.M.L. and D.S. were funded by NIH Grant 2R01GM032741-28. P.P.C. was funded by NIH Grant R01GM36745.

1. Cheng H, Leblond CP (1974) Origin, differentiation and renewal of the four main epithelial cell types in the mouse small intestine. V. Unitarian Theory of the origin of the four epithelial cell types. *Am J Anat* 141(4):537–561.
2. Li L, Clevers H (2010) Coexistence of quiescent and active adult stem cells in mammals. *Science* 327(5965):542–545.
3. Sato T, et al. (2011) Paneth cells constitute the niche for Lgr5 stem cells in intestinal crypts. *Nature* 469(7330):415–418.
4. Kabiri Z, et al. (2014) Stroma provides an intestinal stem cell niche in the absence of epithelial Wnts. *Development* 141(11):2206–2215.
5. Kozar S, et al. (2013) Continuous clonal labeling reveals small numbers of functional stem cells in intestinal crypts and adenomas. *Cell Stem Cell* 13(5):626–633.
6. Potten CS (1998) Stem cells in gastrointestinal epithelium: Numbers, characteristics and death. *Philos Trans R Soc Lond B Biol Sci* 353(1370):821–830.
7. Ritsma L, et al. (2014) Intestinal crypt homeostasis revealed at single-stem-cell level by in vivo live imaging. *Nature* 507(7492):362–365.
8. Snippert HJ, et al. (2010) Intestinal crypt homeostasis results from neutral competition between symmetrically dividing Lgr5 stem cells. *Cell* 143(1):134–144.
9. Lopez-Garcia C, Klein AM, Simons BD, Winton DJ (2010) Intestinal stem cell replacement follows a pattern of neutral drift. *Science* 330(6005):822–825.
10. Yeung TM, Chia LA, Kosinski CM, Kuo CJ (2011) Regulation of self-renewal and differentiation by the intestinal stem cell niche. *Cell Mol Life Sci* 68(15):2513–2523.
11. Oshimori N, Fuchs E (2012) The harmonies played by TGF-β in stem cell biology. *Cell Stem Cell* 11(6):751–764.
12. Baffi MO, et al. (2004) Conditional deletion of the TGF-beta type II receptor in Col2a expressing cells results in defects in the axial skeleton without alterations in chondrocyte differentiation or embryonic development of long bones. *Dev Biol* 276(1):124–142.
13. Forrester E, et al. (2005) Effect of conditional knockout of the type II TGF-beta receptor gene in mammary epithelia on mammary gland development and polyomavirus middle T antigen induced tumor formation and metastasis. *Cancer Res* 65(6):2296–2302.
14. Ito Y, et al. (2003) Conditional inactivation of Tgfbr2 in cranial neural crest causes cleft palate and calvaria defects. *Development* 130(21):5269–5280.
15. Parsons R, et al. (1995) Microsatellite instability and mutations of the transforming growth factor beta type II receptor gene in colorectal cancer. *Cancer Res* 55(23):5548–5550.
16. Grady WM, et al. (2006) Proliferation and Cdk4 expression in microsatellite unstable colon cancers with TGFBR2 mutations. *Int J Cancer* 118(3):600–608.
17. Muñoz NM, et al. (2006) Transforming growth factor beta receptor type II inactivation induces the malignant transformation of intestinal neoplasms initiated by Apc mutation. *Cancer Res* 66(20):9837–9844.
18. Chytil A, Magnuson MA, Wright CV, Moses HL (2002) Conditional inactivation of the TGF-beta type II receptor using Cre:Lox. *Genesis* 32(2):73–75.
19. Biswas S, et al. (2004) Transforming growth factor beta receptor type II inactivation promotes the establishment and progression of colon cancer. *Cancer Res* 64(14):4687–4692.
20. Ficara F, Murphy MJ, Lin M, Cleary ML (2008) Pbx1 regulates self-renewal of long-term hematopoietic stem cells by maintaining their quiescence. *Cell Stem Cell* 2(5):484–496.
21. Snippert HJ, Schepers AG, van Es JH, Simons BD, Clevers H (2014) Biased competition between Lgr5 intestinal stem cells driven by oncogenic mutation induces clonal expansion. *EMBO Rep* 15(1):62–69.
22. Vermeulen L, et al. (2013) Defining stem cell dynamics in models of intestinal tumor initiation. *Science* 342(6161):995–998.
23. Miller AJ, Dudley SD, Tsao JL, Shibata D, Liskay RM (2008) Tractable Cre-lox system for stochastic alteration of genes in mice. *Nat Methods* 5(3):227–229.
24. Fischer JM, Schepers AG, Clevers H, Shibata D, Liskay RM (2014) Occult progression by Apc-deficient intestinal crypts as a target for chemoprevention. *Carcinogenesis* 35(1):237–246.
25. Fischer JM, Miller AJ, Shibata D, Liskay RM (2012) Different phenotypic consequences of simultaneous versus stepwise Apc loss. *Oncogene* 31(16):2028–2038.
26. Barker N, et al. (2007) Identification of stem cells in small intestine and colon by marker gene Lgr5. *Nature* 449(7165):1003–1007.
27. Oshima H, et al. (2015) Suppressing TGFβ signaling in regenerating epithelia in an inflammatory microenvironment is sufficient to cause invasive intestinal cancer. *Cancer Res* 75(4):766–776.
28. Metcalfe C, Kljavin NM, Ybarra R, de Sauvage FJ (2014) Lgr5+ stem cells are indispensable for radiation-induced intestinal regeneration. *Cell Stem Cell* 14(2):149–159.
29. Sato T, et al. (2009) Single Lgr5 stem cells build crypt-villus structures in vitro without a mesenchymal niche. *Nature* 459(7244):262–265.
30. Li HY, et al. (2008) Optimization of a dihydropyrrolopyrazole series of transforming growth factor-beta type I receptor kinase domain inhibitors: Discovery of an orally bioavailable transforming growth factor-beta receptor type I inhibitor as antitumor agent. *J Med Chem* 51(7):2302–2306.
31. Wiener Z, et al. (2014) Oncogenic mutations in intestinal adenomas regulate Bim-mediated apoptosis induced by TGF-β. *Proc Natl Acad Sci USA* 111(21):E2229–E2236.
32. Subramanian A, et al. (2005) Gene set enrichment analysis: A knowledge-based approach for interpreting genome-wide expression profiles. *Proc Natl Acad Sci USA* 102(43):15545–15550.
33. Muñoz J, et al. (2012) The Lgr5 intestinal stem cell signature: Robust expression of proposed quiescent '+4' cell markers. *EMBO J* 31(14):3079–3091.
34. Kim TH, et al. (2014) Broadly permissive intestinal chromatin underlies lateral inhibition and cell plasticity. *Nature* 506(7489):511–515.
35. Falk P, Roth KA, Gordon JI (1994) Lectins are sensitive tools for defining the differentiation programs of mouse gut epithelial cell lineages. *Am J Physiol* 266(6 Pt 1):G987–G1003.
36. Yang Q, Bermingham NA, Finegold MJ, Zoghbi HY (2001) Requirement of Math1 for secretory cell lineage commitment in the mouse intestine. *Science* 294(5549):2155–2158.
37. Canman CE, Tang HY, Normolle DP, Lawrence TS, Maybaum J (1992) Variations in patterns of DNA damage induced in human colorectal tumor cells by 5-fluorodeoxyuridine: Implications for mechanisms of resistance and cytotoxicity. *Proc Natl Acad Sci USA* 89(21):10474–10478.
38. Network TCGA; Cancer Genome Atlas Network (2012) Comprehensive molecular characterization of human colon and rectal cancer. *Nature* 487(7407):330–337.
39. Miyoshi H, Ajima R, Luo CT, Yamaguchi TP, Stappenbeck TS (2012) Wnt5a potentiates TGF-β signaling to promote colonic crypt regeneration after tissue injury. *Science* 338(6103):108–113.
40. Potten CS, Booth D, Haley JD (1997) Pretreatment with transforming growth factor beta-3 protects small intestinal stem cells against radiation damage in vivo. *Br J Cancer* 75(10):1454–1459.
41. Adolph TE, et al. (2013) Paneth cells as a site of origin for intestinal inflammation. *Nature* 503(7475):272–276.
42. Vaishnava S, Behrendt CL, Ismail AS, Eckmann L, Hooper LV (2008) Paneth cells directly sense gut commensals and maintain homeostasis at the intestinal host-microbial interface. *Proc Natl Acad Sci USA* 105(52):20858–20863.
43. Soriano P (1999) Generalized lacZ expression with the ROSA26 Cre reporter strain. *Nat Genet* 21(1):70–71.
44. Mahe MM, Sundaram N, Watson CL, Shroyer NF, Helmrath MA (2015) Establishment of human epithelial enteroids and colonoids from whole tissue and biopsy. *J Vis Exp* (97):52483.
45. Edgar R, Domrachev M, Lash AE (2002) Gene Expression Omnibus: NCBI gene expression and hybridization array data repository. *Nucleic Acids Res* 30(1):207–210.
46. Ewens WJ (2004) *Mathematical Population Genetics 1: Theoretical Introduction* (Springer-Verlag, New York), 2nd Ed.